Modeling, Design and Simulation of Bicycle Anti-Theft Device

Carlos A. Toledo, Daniel S. Gordillo, and Diego J. Sánchez
Francisco José de Caldas Distrital University, Engineering Department, Bogotá D.C., Colombia
Email: catoledob@udistrital.edu.co, dsgordillom@correo.udistrital.edu.co, djsanchezr@correo.udistrital.edu.co.

***Abstract* — In recent times, the bicycle has become one of the most important means of transportation in cities presenting a large amount of traffic jams. Unfortunately, the major growth of cycling has led on to a directly proportional increase in different social problems. Bicycle theft along with lack of confidence when riding due to insecurity in great cities could impede the encouragement of bicycles as the main mode of transport and thus achieve sustainable mobility. This article will discuss the possibility of designing and simulating an engineering solution that will mitigate the social problems of bicycle theft, focused on a particular modality such as robbery. The proposed solution will consist of the development of a mechanical device composed of a mass-spring system that will instantly block the natural movement of the front wheel, causing a partial immobilization of the bicycle. Said immobilization will allow the cyclist to recover the vehicle after experiencing the robbery. The results of the simulations run with the CAM SolidWorks software, by way of tools such as SolidWorks Simulation, and Motion Study, allowed to validate the mathematical models of mechanical stresses and displacements resulting from the impact between the wheel and the device. Likewise, the dimensions and characteristics of the mass-spring system were also verified. At the end of the article, the appropriate materials for the different components will be determined in order for them to be manufactured, and the future works to be realized will be identified.**

***Index Terms*—CAD/CAE, design and simulation, SolidWorks, bicycle, sustainable mobility, anti-theft device.**

I. Introduction

The increasing use of bicycles as a means of transportation in cities has been accompanied by different social problems, one of them being the insecurity that affects cyclists. There is a strong correlation between the great acceptance of the bicycle as an alternative mode of transport, and the increase in bicycle theft.

Reference [1] Only in Bogotá Colombia, 835,000 inhabitants use the bicycle to circulate; yet, according to some statistics from the District Secretary of Security, Coexistence, and Justice of the Bogotá Mayor's Office, 4,628 bicycle thefts occurred in the city between January and December 2017. Whereas, between January and December 2018, there were 7,919 cases, that is, the theft of bicycles increased by 71.1% in one year. [2]

For this reason, researchers and authorities pursue various solutions to mitigate this social problem, which has even caused deaths: 15 cyclists died in the first three months of 2019 [3]. With the implementation of an anti-theft device, the aim is to reduce the number of bicycle thefts, since 4 out of 10 of them operate under the robbery modality [4]. In this article, an engineering solution is proposed by way of a mechanical device composed of a mass-spring system which will partially block the operation of the bicycle, thus preventing its theft when the cyclist is using it. The rest of the article will be structured as follows. Section II presents the literature review on similar systems. Section III describes the design, components, and operation of the device. Section IV provides the mathematical models that were used to analyze the general behavior of the device; and so be able to determine the stresses and speeds to which it will be subjected when blocking the operation of the bicycle. Section V depicts the impact and displacement simulations performed to the constituent components of the anti-theft device, through various tools provided by CAM SolidWorks Software. Finally, section VI presents the conclusions and future work to be realized.

II. Background

A. Literature Review

In order to elaborate the conceptual design of a bicycle anti-theft device, it was necessary to identify the two most common forms of bicycle theft. Through a literature review, the authors came to the realization that there exist two main forms of theft: the bicycle theft when they are parked, and theft when the driver uses the vehicle.

It was also found that most bicycle anti-theft systems are designed using only electronic systems; monitoring and tracking of the bicycle by means of GPS tools taking great value.

The literature review showed no bicycle anti-theft device similar to the one proposed in this project; however, solutions that address the problem of bicycle theft in a way differing from the proposal presented in this article were observed.

Firstly, a device that informs the cyclist in the event of theft was identified. When the bicycle is left parked and it tries to be moved or stolen, it sends a message to the

Manuscript received September 7, 2019; revised October 11, 2020.

doi: 10.18178/ijmerr.9.11.1463-1473

cyclist's cell phone informing the situation, in addition to emitting a sound of alert [5].

A device known as NaviRide similar to the previous one, but providing a tracking system, was developed. When the bicycle is stolen, it sends the coordinates of its location to the owner’s cellphone via text message. It also features a collision-detection system, so in the event of traffic accidents, the device will transmit messages informing of the emergency [6].

On the other hand, in Japan an IOT device for bicycles was developed, which links the bicycle to the owner's smartphone; once it is parked its location can be monitored. After the bicycle is stolen and moved from the parking area, the device turns on and sends a message to the owner, informing him of the movement. He is able to check the current position of the bicycle and the route it follows so as to reach that new location; afterwards, the owner can decide whether to send a message with the bicycle’s whereabouts and the route taken by the offender, reporting the situation to the competent authorities [7].

The team also found an electronic device consisting of a microcontroller, sensors, and actuators. It fulfills the function of protecting the bicycle against theft when it is parked. The system consists of a keypad, upon which one must enter a password, a proximity sensor, and an alarm. Thus, when the offender approaches the bicycle, the proximity sensor turns on, which causes it to activate the alarm that reports the theft, said alarm is not deactivated until the password is entered [8].

A different approach to preventing bicycle theft was creating a system known as SaveMyBike, which will provide specialized secure bicycle-parking spaces at different points in the cities. It aims to delimit these areas and protect bicycles that can be parked there, by means of alarms, and RFID signals. If the bicycle were to leave the parking area forcibly, the areas surrounding the parking lot would be able to track the position of the bicycle using RFID technology. Once the bicycle is tracked, a police officer can locate it and confirm if it is the stolen bicycle, by scanning the code printed on the bicycle’s frame with the RFID reader [9].

As the reader may observe, most solutions are based on electronic devices installed on the bicycle, and, although they try to prevent the theft of these vehicles, they focus on cases taking place when the bicycle is parked, none of them addresses to avoiding bicycle theft that occurs when the rider is riding and it is forcibly taken from him.

III. METHODOLOGY

A. General Design

This article focuses on looking for a possible solution to the social problem of bicycle theft, fixing the attention on a particular form of theft: robbery. For this purpose, the conceptual design of the anti-theft system had to identify all the variables involved in this theft modality, the analysis showed that the act of instantly stopping, blocking, and immobilizing the bicycle is a possible solution. Based on this requirement, the critical points of the bicycle that may give place to a partial or total failure in its operation were identified. Fig. 1 shows the critical points of the bicycle.

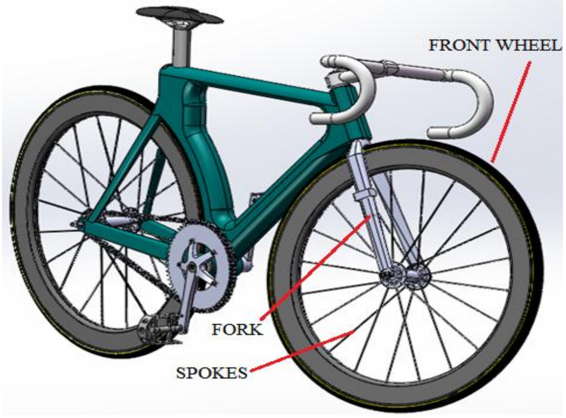

Figure 1. Critical points of the bicycle.

Consequently, the analysis concluded that the directional wheel, that is, the front wheel, was one of the most critical points due to its importance for driving inertia; and the possible forms of failure of this critical point were determined. Once the best conceptual design was selected, the research team developed the preliminary design of the device based on the possible failures of the front wheel. It was established that the anti-theft device should be located on the fork to cause a lock on the front wheel of the bicycle. To create this type of lock, and by the aid of the fork as a support, the authors devised and designed a way in which the fork and the wheel produced direct contact between them, thus interfering with the right operation of the bicycle.

This design consists of deploying an element in a controlled way when the bicycle is in motion and at a certain speed, which must pass through the spokes of the wheel until it reaches the other fork’s arm, generating the blockage. For this preliminary design, the shape, dimensions, and operation were determined, without leaving aside user requirements such as aesthetics, and degree of interference in driving. Fig. 2 shows the initial position of the bicycle anti-theft device and how it should be located on the rear of the fork.

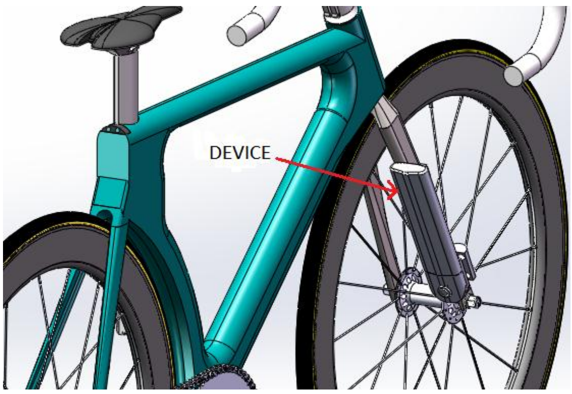

Figure 2. Device starting position.

The final position of the device is shown in Fig. 3, successfully blocking the front rim.

Figure 3. Device final position.

B. Components

The computer-aided design (CAD) models of the components to be analyzed must be fashioned in detail previous to the running of any simulation. The components of the bicycle anti-theft device are shown below in Fig. 4 and Table I. They were modeled with the help of CAM SolidWorks 2018 software [10].

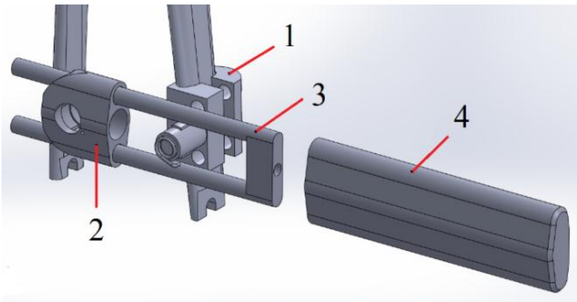

Figure 4. Anti-theft device components.

TABLE I. COMPONENTS ANTI-THEFT DEVICE

Id.	Name
1	Adjustable clamping system with fork
2	Turning system
3	Rods
4	Cover or case

B.1 Adjustable Clamping System with Fork

This clamping system will provide the necessary grip between the device and the bicycle's fork arm with the help of two screws (with special heads for greater security), thus guaranteeing that the system remains in the determined position. Likewise, the system will also hold the rest of the components charged with potential energy at all times. The internal dimensions of this component will in turn depend on the fork's size and type; the fork examined in this case was taken from a conventional racing bicycle. Fig. 5 shows in more detail the Id.1 component with its main parts: the initial release ratchet, the retractable bolts, and the torque spring.

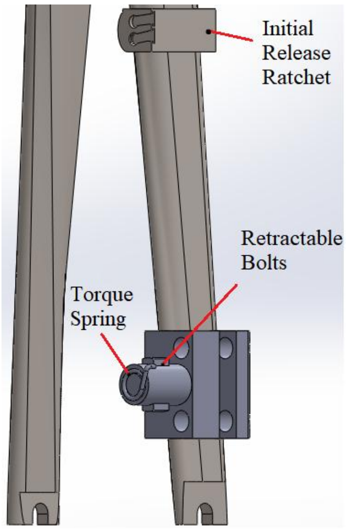

Figure 5. Adjustable clamping system with fork.

B.2 Turning System

The Id.2 turning system will be coupled together with the Id.1 clamping system, which will produce an angular shift of 90 degrees, achieving a change from the initial position (*see* Fig. 2) to the final position (*see* Fig. 3) by the aid of the torsion spring of component Id.1, thus preparing it for the release of the rods. Fig. 6 shows where the torsion spring will be connected to the turning system, and also, where the secondary release ratchets are located.

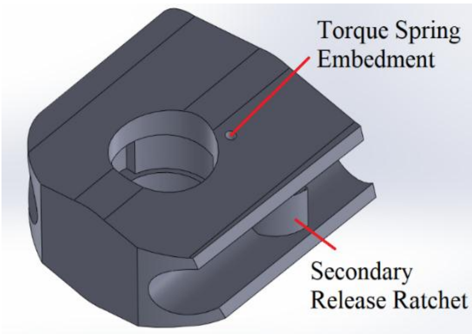

Figure 6. Turning system section view.

B.3 Rods

This is the most important component of the anti-theft system, since it will have to absorb the impact and lock the wheel of the bicycle. Fig. 7 shows how it is designed so that it be a one-piece element.

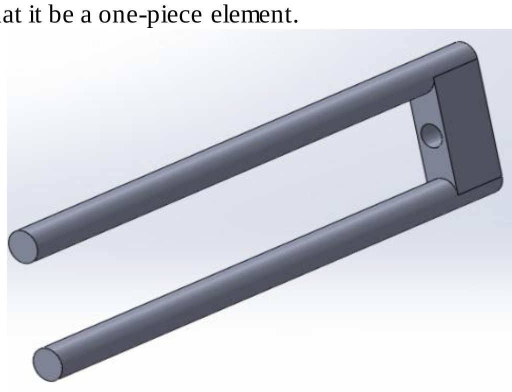

Figure 7. Rods.

B.4 Cover or Case

This component, in addition to satisfying the user's aesthetic requirement, will protect the rods from intrusive elements that might interfere with the right operation of the anti-theft device. Fig. 8 shows the mechanical pins that will hitch component Id. 1 (*see* Table I) to hold the device in its initial position.

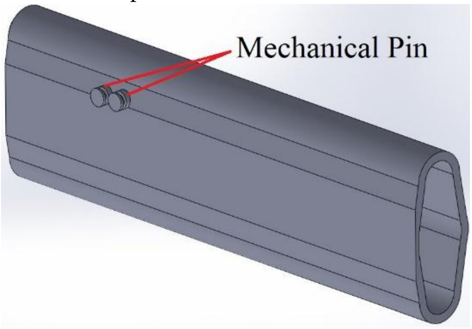

Figure 8. Cover or case.

C. Operation

The operation will consist of 4 phases, shown below.

C.1 Activation Phase

This phase will depend entirely on the action, reaction time of the cyclist, and the speed of the bicycle, as the cyclist is the one who will decide whether to remotely activate the device through the electronic system or not. The mechanical pins in component Id. 4 (see Fig. 8) are uncoupled from the initial release ratchet in component Id. 1 (see Fig. 5). Said process will be controlled electronically, and by means of an electronic odometer, which will compute the speed of the bicycle, deciding if the ratchet is to be activated or not; if the speed is faster than 1.38 m/s this phase will not take place.

C.2 Rotation Phase

This phase will control the change of positions. When the activation phase begins, the initial position will change, then the torsion spring of the Id.1 component will cause the Id.2 component to rotate. As seen in Fig. 9.

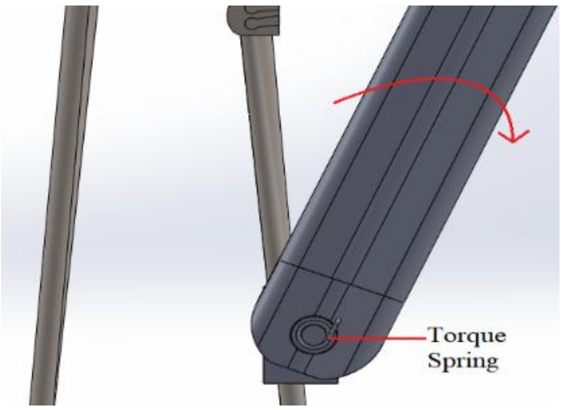

Figure 9. Torsion spring turning the device.

The final position will be reached when the 90-degree angle spin be achieved and it be in a restricted position, perpendicular to the fork. In order to retain this position, Id.2 component will be fitted to the retractable locking bolts located in component Id. 1 (*see* Fig. 5). Fig. 10 (a) shows how the bolts are retracted in the initial position, allowing rotation of component Id.2. In (b) the locking bolts return to their initial position enabling embedment.

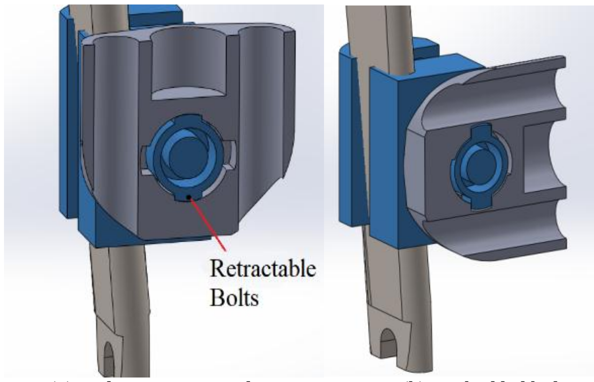

(a) Bolts are retracted. (b) Embedded bolts.

Figure 10. Rotation phase of the anti-theft device.

C.3 Deployment Phase

The deployment phase is the main phase of the system's operation, since a correct deployment will depend on the effectiveness of the bicycle anti-theft system. This phase begins when the final position is reached, (*see* Fig. 10 (b)). The embedment has a double functionality: the first being to preserve the mechanical part's perpendicular position in relation to the fork; the second one, to start up the electronic system that will activate the secondary release ratchet of component Id. 2 (*see* Fig. 6), releasing in turn the component Id. 3 charged by the elastic potential energy of the main tension spring, as seen in Fig. 11. This phase will end when the component Id. 3 have passed entirely through the spokes of the wheel and reached the other fork's arm.

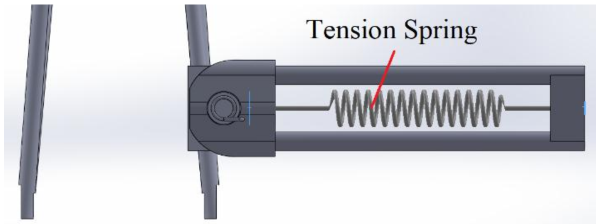

Figure 11. Rods loaded with elastic potential energy.

C.4 Impact Phase

In the impact phase, component Id. 3 will withstand, together with the fork arms, all of the spokes' impact load, causing an interference and stopping the natural movement of the front wheel, and so, producing a partial lock of the bicycle. The selection of the material used for this component will be explained in detail in the following sections.

IV. Mathematical Model

A. Resulting Impact on Rods

In order to know how feasible the proposed device is, and given the dynamic behavior of its operation, the physical concept of impact loading was used. It is the most suitable one for determining the activity to which the device will be subjected, specially the rods, as they will receive the full impact.

The concept of impact loading establishes that, in a dynamic system, the maximum deformation that a beam undergoes due to the impact of a body carrying a determined kinetic energy, may be equivalent to a static system through a point load.

Once the operation and behavior of both the device, and the bicycle is known, it should be understood that, when the spokes of the bicycle's front wheel collide with the rods, the kinetic energy carried by the former, due to the bicycle's speed and mass, becomes deformation energy on the rods, producing bending stresses in them.

The work performed by a load P, when slowly applied to the beam, must result in an increase of energy associated to the deformation in the latter; in this case, the rods of the device. That energy is the beam's deformation energy, which is the area comprised between $x = 0$ and $x = x_1$ under the load (N)-deformation (m) curve.

Knowing that the deformation energy is the area under the load-deformation curve, the maximum value of the stress suffered by the beam at a specific point in the structure subjected to the impact load must be determined, this will allow establishing the type of material to use. In order to do so, it will be assumed that the kinetic energy of the body that hits the beam is transferred entirely to the structure, i.e., that all the energy generated by the impact will be absorbed by the rods and will become deformation energy. In practice, this does not happen, and only a portion of the energy is transferred to the rods, which means that a conservative design of the rods will be obtained [11].

Hence, the strain energy U is calculated with (1), where P corresponds to the applied load.

$$U = \int_0^{x_1} P\,dx. \tag{1}$$

In the case of a linear and elastic deformation, the portion of the load-deformation diagram, where only elastic deformation occurs, can be represented with a straight line where $P = kx$. Substituting P and integrating in (1), we obtain (2), where P_1 is the value of the load corresponding to the deformation x_1.

$$U = \frac{1}{2}\ P_1\, x_1. \tag{2}$$

The energy carried by the bicycle before impact, which will be the same energy that the rods must absorb, is calculated with (3), where Ec is the kinetic energy, m is the addition of the rider's mass plus the bicycle's, and v is the bicycle's speed before impact.

$$Ec = \frac{1}{2}\ mv^2 \tag{3}$$

Now then, when a structure is subjected to a single concentrated load, it is possible to use (2), and, depending on the beam's supports, and the point upon which the load is applied, the deformation x will take the value of the deflection of each type of beam in particular. In summary, the energy of deformations is equal to the product of the average force and the deflection [12].

For this specific device, the rods must be propelled out and rest completely on the other fork's arm, thus resembling a beam with two supports. Additionally, the spokes of the wheel will be assumed to impact exactly in the middle of the device's rods and to transfer an amount of energy equivalent to a mass of 95 kg (80 kg, average weight of a man + 15 kg, average weight of a bicycle) moving at a maximum speed of 1.38 m/s.

Consequently, the impact system will be similar to Fig. 12, where the moving object will be the spokes of the rims of the bicycle's front wheel, the beam will be the rods of the device, and the supports will be the arms of the fork.

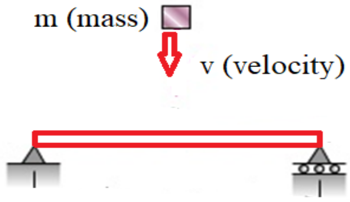

Figure 12. Support type of rods before impact.

The deflection for this beam configuration is given with (4), this value will take the value of x in (2). Where P is the applied load, L is the length of the rods, I moment of inertia and E modulus of elasticity [13].

$$x = deflexion\ = \frac{PL^3}{48EI} \tag{4}$$

The moment of inertia I is calculated with (5) where $Rexternal$ y $Rinternal$ are the external and internal radius of the rods' profile, respectively.

$$I = \frac{Rexternal^4 - Rinternal^4}{4} * \pi \tag{5}$$

The maximum stress $(\sigma)_{max}$ for the configuration shown in Fig. 12. It is calculated with (6) where P is the applied load, L is the length of the rods, I moment of inertia and c distance from the neutral axis to the farthest fiber.

$$(\sigma)_{max} = \frac{P*L*c}{4I} \tag{6}$$

The dimensions, the material and the stress to which the rods of the device will be subjected are then calculated.

Parameters

- Total mass (m) = bicycle mass + cyclist mass = 15 kg + 80 kg = 95 kg.
- Speed (v) = 1.38 m/s.
- Rod length (L) = 0.2 m, fork's arm spacing.
- Rod profile = circular
- Elasticity module (E) = the rod will be from the steels' family = 2.07 $x10^{11}$ PA
- $Rexternal$ = 0.006 m y $Rinternal$ = 0 m
- c (distance from the neutral axis to the farthest fiber) = 0.006 m.

Once having the parameters and variables to be used, the calculations are carried out. Taking (3) is calculated Ec.

$$Ec = \frac{1}{2}\,(95\ kg) * (1.38\ {}^{m}/_{s})^2 \ = \ 90.12\ \mathrm{J}$$

Taking (5) the moment of inertia I is calculated.

$$I \ = \ 1.01788x10^{-9}m^4$$

Replacing (4) in (2) and solving for *P*, we obtain the equivalent load (force) of the kinetic energy at the moment of impact. Thus, (7) is determined, where the deformation energy *U* of the rods is equal to the kinetic energy resulting from the impact.

$$P = \sqrt{\frac{96UEI}{L^3}} \tag{7}$$

Substituting values in (7) we obtain.

$$P = \sqrt{\frac{96 * 90.12J * 2.07\ x10^{11}\,PA * \ 1.01788\,x10^{-9}m^4}{(0{,}2m)^3}}$$

$$P = 15095.61\ \mathrm{N}$$

Since the design is composed of two rods, both of them receiving the impact, and both behaving as shown in Fig. 12, each one will undergo a load of *P/2*, that is, 7547.80 N.

The maximum stress $(\sigma)_{max}$ that each rod will experience is next calculated. Taking (6) and replacing the values we obtain:

$$(\sigma)_{max} = \frac{7547.80N * 0.2m * 0.006m}{4 * 1.01788\,x10^{-9}\ m^4}$$

$$(\sigma)_{max} = 2.22\ \mathrm{x}10^9\ \mathrm{PA}$$

The material that will endure said maximum stress $(\sigma)_{max}$ is then chosen. As it is such a high stress, type S steel ought to be used, this sort of steel is impact resistant; and is used in applications requiring high toughness, and resistance to impact load. Therefore, S5 steel is selected, which has a yield strength of 1900 MPa, and an ultimate strength of 2300 MPa [14]. Consequently, the material and dimensions of each rod should be:

- Material = S5 steel
- External diameter = 0.012 m
- Internal diameter = 0 m

Taking these specifications into account, the rods will theoretically present permanent deformation. That being the case, we want to clarify that the main objective of the anti-theft device is to lock and stop the wheel, despite the fact that the rods suffer permanent deformation, hence, maximum stress $(\sigma)_{max}$ is not compared to yield strength since the rods will be for single use only.

B. Design of the Tension Spring

The type of spring to be used is a tension spring, (*see* Fig. 11). This will be the main spring; whose function is to move the rods at a given speed. To determine the value of the spring constant *k*, we will use (8), where *m* is the mass of the rods, *v*, the speed at which the rods will move, and *A*, the stretch of the spring.

$$\frac{1}{2}\,mv^2 = \frac{1}{2}\,kA^2 \tag{8}$$

Equation (8) states that the elastic potential energy, present in the spring when it is stretched or compressed, must be converted into kinetic energy when the spring is released under tension, causing the rods to move at a speed *v* [15].

The mass *m* is obtained from the SolidWorks software, after placing the S5 Steel material on the rods. The value is 0.337 kg.

The speed *v* must guarantee that the rods successfully traverse the wheel of the moving bicycle. Using the tracker software, the speed was measured by analyzing three videos taken off a trigger in action, which managed to cross the bicycle's wheel that rotated at an average speed of 4.2 m/s.

Fig. 13 shows the maximum speed of a projectile that successfully passed through the front wheel of the bicycle in three different attempts.

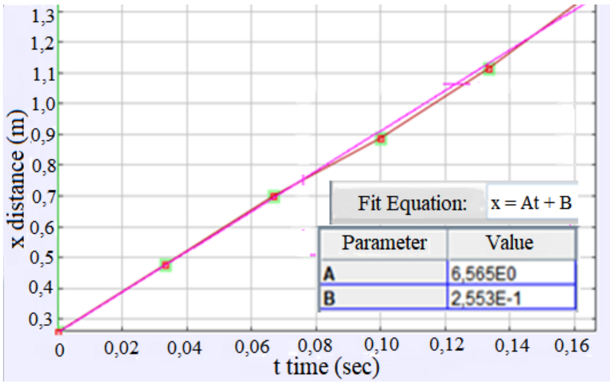

Figure 13. The magnitude of the speed was 6.56 m / s.

It was concluded that the speed *v* necessary for the projectile to successfully block the wheel should be 6.56 m/s, deciding to round to 7 m/s for a greater probability of success.

The stretch of spring *A* will be 0.11 m, restricted by the dimensions of the device. Taking (8), replacing values, and solving for the spring constant *k*, we obtain *k* = 1364.7 N/m. Knowing the value of the constant, the spring is designed. *K* is defined as the variation of the load *F* per unit of deflection δ. This can be calculated with (9), where *G* is the shear modulus of material, *d*, spring wire diameter, *D*, outer diameter of spring, and n_a, number of active coils [16].

$$k = \frac{Gd^4}{8D^3 n_a} \tag{9}$$

Parameters:

- Shear modulus of material (G) = On average the value of *G* for the most common materials in springs is 79 GPa [17]
- Outer diameter of spring (*D*) = 0.015 m
- Number of active coils (n_a) = 20

Substituting and solving for d in (9), we obtain. Spring wire diameter d = 0.001747 m. The length of the spring will be 0.035 m, as shown in Fig. 14.

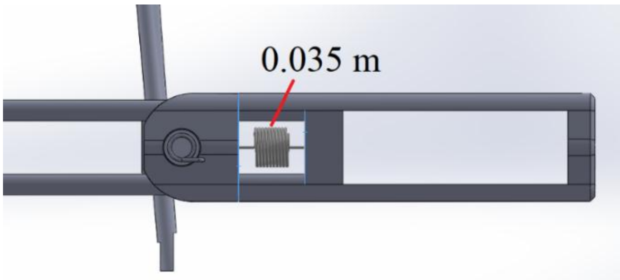

Figure 14. Tension spring length.

V. SIMULATIONS

A. Impact Simulation

Reference [18] through an analysis using the finite element method (FEM), which allows corroborating the maximum stress, deformations, and displacements that elements or structures experience when subjected to various mechanical loads, the aim is to validate the developed mathematical model and determine the maximum von Mises stress that the rods of the bicycle anti-theft device will experience when subjected to impact loads. Reference [19] the FEM is based upon the assumption that any geometry can be decomposed into discrete elements having small areas or volumes. SolidWorks Version 2018 software was used to perform the FEM study on the rods that will receive the full impact, the results are presented below. This simulation will analyze only component Id. 3, (*see* Table I).

First, the stage shown in Fig. 15 is assembled. Piece 1 corresponds to the device's rods, to which the material S5 steel is assigned. Piece 2 represents the object that will impact the rods, it aims to simulate the energy that the bicycle will carry at the moment of impact, therefore, said object has a mass of 80 kg and will move at a speed of 1.5 m/s, which is equal to a kinetic energy of 90 J.

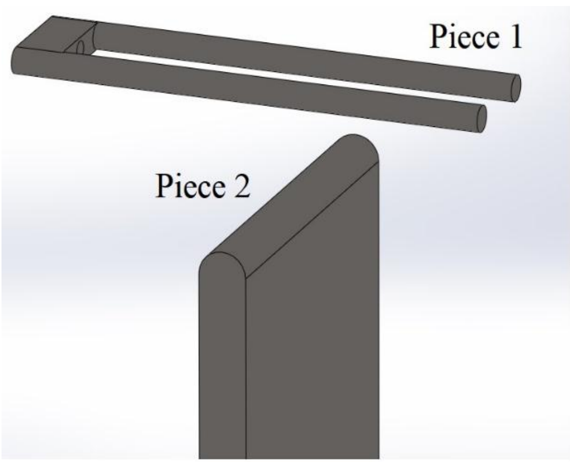

Figure 15. Assembly made before the simulation.

The SolidWorks Simulation tool ran the simulation following a non-linear-dynamic study.

In linear static analysis, loads are gradually and slowly applied, until they reach their maximum magnitude; after reaching this point, the charges remain constant. The accelerations and speeds of the system are considered insignificant. In a dynamic analysis, the loads depend on the time; thus, in a very short time, the entire load might be applied, which would be considered an impact load; the speeds and accelerations of the system also become highly important in the study. Non-linear analyzes take into account those significant changes that objects can suffer due to loads, undergoing permanent deformations. [20]

The initial conditions of the simulation are depicted below. Piece 1 was assigned a fixed clamp at each end as shown in Fig. 16. Piece 2, simulating the mass of the bicycle and the cyclist, was provided with the speed at which it should be moved. Additionally, it is stated that the object is rigid, therefore it will not present deformations: by doing so, it is assumed that the anti-theft device will absorb the whole impact energy. In the connections, it is indicated to the software that there will be no penetration between piece 1 and piece 2.

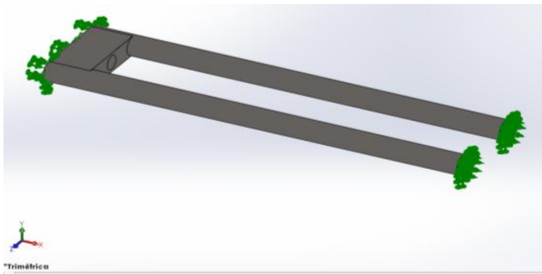

Figure 16. Types of fasteners.

The distance at which both pieces must be placed before running the simulation is 1.5 m, since the simulation runs for a 1-second time span. So, if the object moves at a speed of 1.5 m/s, that means that it will hit the rods in that time span.

After running the simulation, the following results were obtained.

Fig. 17 shows the result of the maximum stress that the rods of the anti-theft device will withstand after receiving an impact equivalent to 90 J. This value is 2200 MPa.

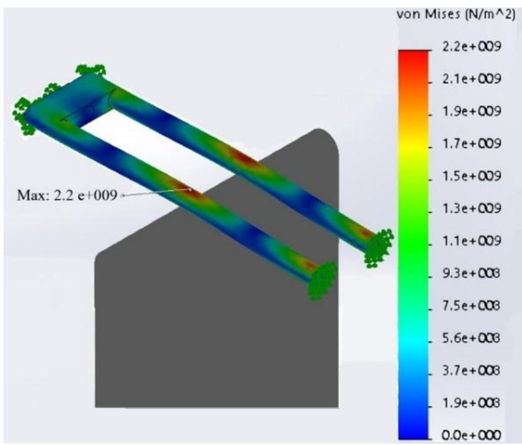

Figure 17. Stress caused by impact.

Fig. 18 shows the result of the maximum displacement that the rods of the device will have after impact. This value is 0.003 m and occurs in the middle of the rods, just where the impact is received from the wheel spokes of the bicycle.

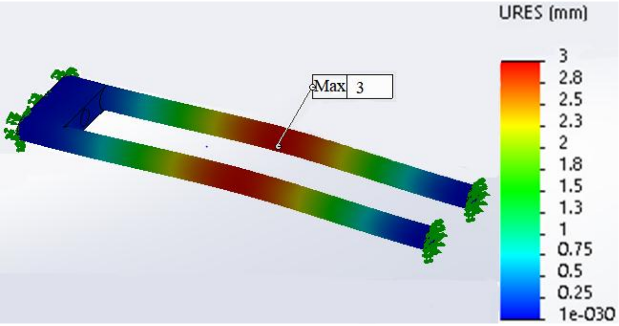

Figure 18. Displacement caused by impact.

B. *Tension Spring Simulation*

SolidWorks software and its motion study tool were used in order to simulate the tension spring earlier designed. The mentioned program allows adding motion to the components of an assembly, evaluating the correct operation of the mechanism, as well as simulating effects with motors, contacts, gravity, and springs [21].

Fig. 19 shows the spring's parameters needed to run the motion study, which are its spring constant, free length, outer diameter, number of active coils, and the spring's wire diameter.

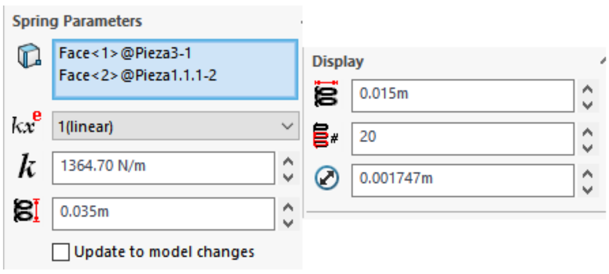

Figure 19. Spring parameters.

Then the spring is stretched as shown in Fig. 20, extending it 0.11 m, thus going from a length of 0.035 m to one of 0.145 m.

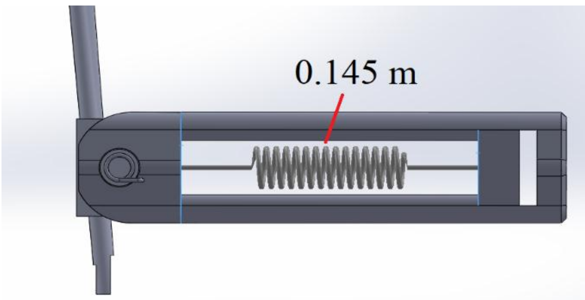

Figure 20. Spring stretch.

After executing the motion study, the speed at which the spring moves the rods was obtained, as observed in Fig. 21, this speed is 7 m/s.

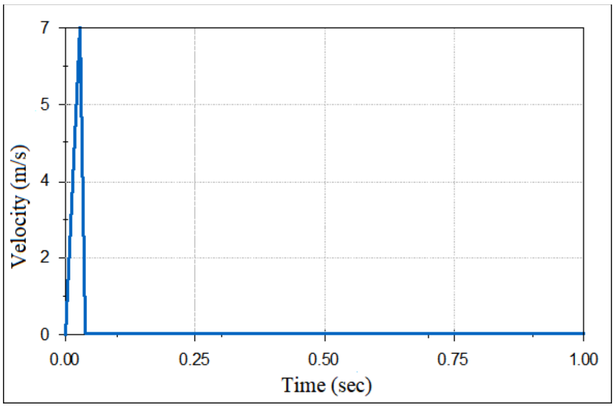

Figure 21. Speed at which the rods move.

C. *Assemble Simulation*

For observing the behavior of the other parts of the anti-theft device, the software ran another simulation, having the same characteristics as the previous one, that is, an object carrying an energy of 90 J hit the device. The only different element was the addition of the contacts, for which no penetration between each one of the pieces should be allowed. Each component was assigned an initial material. The results obtained are:

- Component Id.1, (*see* Table I). Material: 1060 aluminum alloy.

Fig. 22 show maximum stress of 150 MPa obtained.

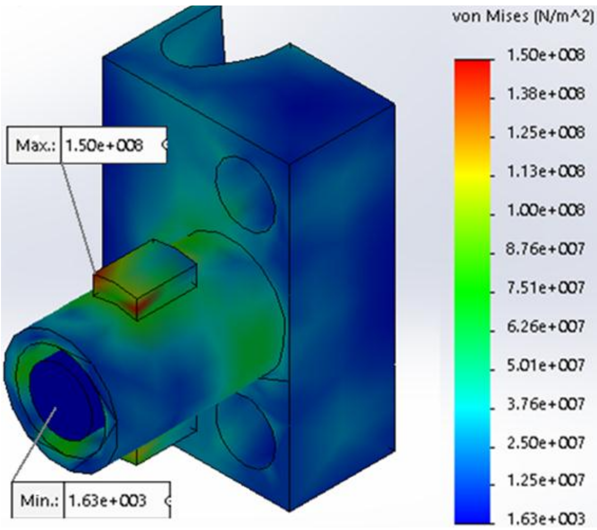

Figure 22. Maximum stress on adjustable clamping system with fork.

The Material Properties are, yield strength = 27 MPa, ultimate strength = 68 MPa. Thus, since yield strength is less than the maximum stress, it is necessary to change the material.

- Component Id. 2, material: 1020 Steel, cold rolled.

Fig. 23 shows the maximum stress obtained: 126 MPA.

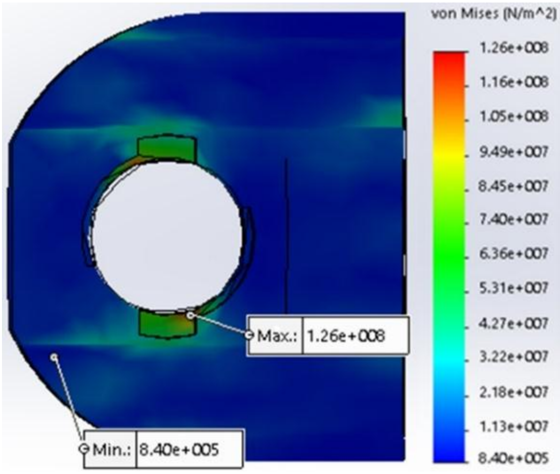

Figure 23. Maximum stress on turning system.

The properties of the material are yield strength = 351 MPa, ultimate strength = 420 MPa.

Considering that a material with lower density might be found in order to decrease the weight of the device, among other reasons, it is necessary to look for another material with a yield strength closer to the maximum stress of the component Id.2

- Component Id. 4, material: rigid PVC

Fig. 24 shows the maximum stress obtained: 3.18 MPa.

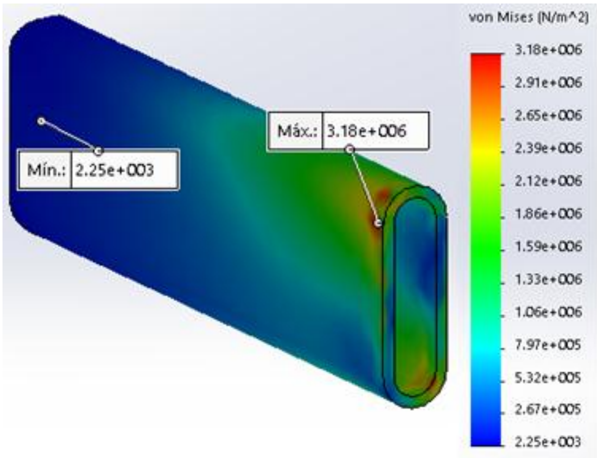

Figure 24. Maximum stress on cover or case.

The material properties are ultimate strength = 40 MPA. Therefore, by comparing both values, it was decided to preserve the material.

With the information from the previous simulation, the materials of component Id. 1 and Id. 2 were changed and the simulation was run again. For Id. 1, the material was changed to AISI 304 stainless steel, it has good properties such as resistance to corrosion, and it is mainly used in the food, beverage and automotive industries. Yield strength and ultimate strength values are, respectively, 206 MPa and 515 MPa [22].

After modifying the material, the simulation produced the following results. Fig. 25 shows the maximum stress on component Id.1.

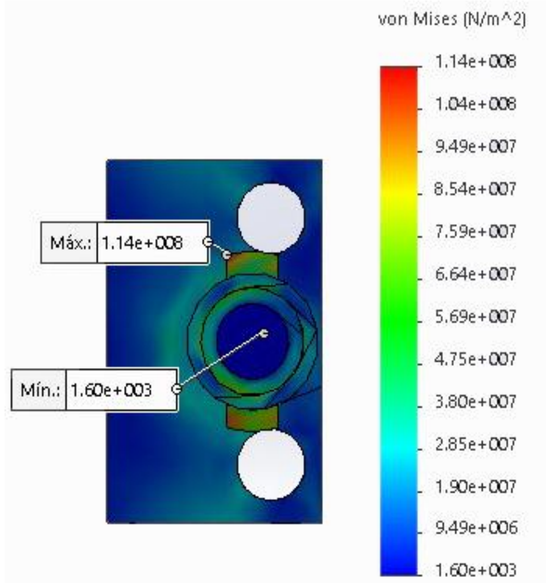

Figure 25. Maximum stress on adjustable clamping system with fork.

The maximum stress is 114 MPa; which is less than the yield strength, therefore, the material will not undergo permanent deformation.

For component Id. 2, the material was changed to a 6/10 nylon plastic. This thermoplastic is used in many engineering applications as it offers a combination of high mechanical strength, heat resistance, and low density. This plastic is characterized by having a region of linear elastic deformation, later, a plastic region where it will present permanent deformation [23]. Its yield strength and ultimate strength values are 139 MPa and 142 MPa, respectively.

After modifying the material, the following results were obtained. Fig. 26 shows maximum stress on Component Id.2.

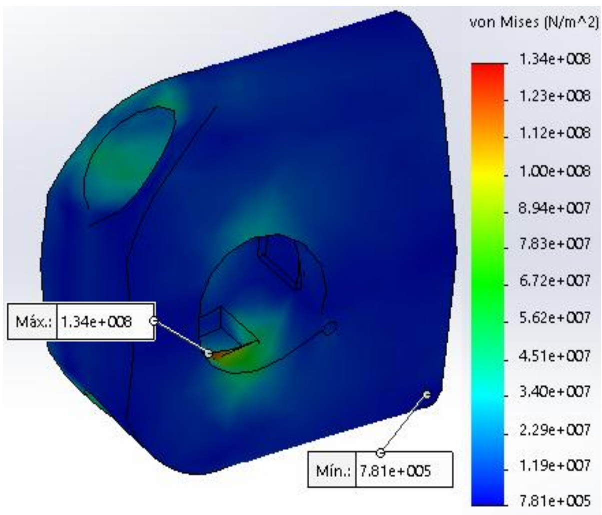

Figure 26. Maximum stress on turning system.

The maximum stress is 134 MPa. Since it is less than the yield stress, the material will not undergo permanent deformation.

VI. Conclusion and Future Works

It was found that most bicycle anti-theft devices are focused on preventing theft when the bicycle is parked, however, it is also important to consider the thefts operating under robbery modality. The design proposed in this article was proved to be feasible and likely to help mitigate this type of theft.

It was demonstrated, both theoretically and experimentally, through SolidWorks Simulation tool, that the impact, equivalent to 90 J, will produce a maximum stress of 2200 MPA, and a maximum permanent displacement of 0.003 m in the rods (*component Id.3*). The stresses, as well as the displacements, occur in the longitudinal half of the rods, right where the spokes of the wheel receive the impact. As it is such a great stress, a type S steel must be used; this is a kind of impact-resistant steel. The final selection was using S5 steel, which has a yield strength of 1900 MPa, and an ultimate strength of 2300 MPa.

The dimensions and the elasticity constant of the tension spring were determined mathematically, and by means of simulation through the SolidWorks software, specifically, with the help of the Motion Study tool. The spring constant k must be equal to 1364.7 N/m; outer diameter, 0.015 m; wire diameter, 0.00174 m; and length, 0.035 m. With these dimensions it is guaranteed that the spring is able to propel the rods at a speed of 7 m/s, and to successfully traverse the spokes of the front wheel, when the bicycle presents a maximum speed of 1.38 m/s.

Finally, it was possible to determine the maximum von Mises stresses resulting from the impact equivalent to 90 J in each of the other components of the device, by means of impact simulations run by the SolidWorks Simulation tool. This, in turn allowed determining the appropriate materials, shown in Table II, so that these components do not be permanently deformed.

TABLE II. Components' Materials

Id.	Name	Maximum stress (MPa)	Yield stress (MPa)	Material
1	Adjustable clamping system with fork	114	206	AISI 304
2	Turning system	134	139	Nylon 6/10
4	Cover or case	3.18	-	Stiff PVC

Future works aim to develop the electronic system that allows remotely activating the mechanical components of the device presented here. Additionally, a prototype will be built based on the determined materials and the anti-theft device will be tested in real conditions, in order to validate the conclusions exposed in this article. Ultimately, the device will be presented to cyclists to gather suggestions for possible improvements on its development, based on which, everything will be incorporated, and a final prototype will be built together with its part plans for mass manufacturing.

Conflict of Interest

The authors declare that there is no conflict of interests regarding the publication of this paper.

Author Contributions

Carlos A. Toledo contributed to the monitoring, validation of results and final editing of this research work; Diego J. Sánchez contributed with the mechanical design and operation; Daniel S. Gordillo contributed with the theoretical formulation and simulation. In general, all authors approved the final version.

Acknowledgment

This research work was supported by the DIMSI (Design, Modeling and Simulation) research group of the engineering faculty of the Francisco José de Caldas Distrital University.

References

[1] Portafolio, "68% of trips made by bike in Bogota are for work," Portafolio, 1 July 2018.

[2] District Secretary of Security, Coexistence and Justice of Bogota, "Bicycle Theft Statistics," Bogota, 2019.

[3] J. D. Rodriguez, "Bicycle theft in Bogota has increased 400% in three years," La FM, 12 April 2019.

[4] Bogota how we are doing, "Security for bicycle users," February 2019. [Online]. Available: https://bogotacomovamos.org/seguridad-para-los-biciusuarios/. [Last access: July 2019].

[5] H. Jialiang, L. Mengzhuo, W. Yunman, and X. Zhiqiang, "Design of an intelligent bicycle safety driving system," *Safety Science*, vol. 118, pp. 397-402, 2019.

[6] P. Dutta and U. S. G. V. Dontiboyina, "NaviRide: Smart bicycle computer with GPS waypoint," presented at the *Second International Conference on Computational Intelligence & Communication Technology (CICT)*, Ghaziabad, 2016.

[7] M. Saegusa and K. Katsura, "Development of a smart IoT device for bicyclists," presented at the *7th International Conference on Integrated Circuits, Design, and Verification (ICDV)*, Hanoi, 2017.

[8] N. Amin, T. Ahmed, S. M. Olee, M. T. Alam, and T. Kaisar, "Technologically enhanced bicycle: anti-theft security, automated gear system and rear protection," presented at the *10th International Conference on Electrical and Computer Engineering (ICECE)*, Dhaka, 2018.

[9] M. Petri, M. Frosolini, M. Lupi, and A. Pratelli, "ITS to change behaviour: A focus about bike mobility monitoring and incentive — The SaveMyBike system," presented at the *16th International Conference on Environment and Electrical Engineering (EEEIC)*, Florencia, 2016.

[10] P. Bhaveshkumar Y J. Prajapati, "Static analysis of mini hydraulic backhoe excavator attachment using FEA approach," *International Journal of Mechanical Engineering and Robotics Research*, vol. 1, no. 3, pp. 163-175, 2012.

[11] F. Beer, R. Johnston, J. Dewolf, and D. Mazurek, "Energy methods," *Mechanics of Materials*, Fifth ed., Mexico DF, McGraw Gill, 2009, pp. 669-726.

[12] R. Budynas and K. Nisbett, "Deflection and stiffness," *Shigley´s Mechanical Engineering Design*, Eighth ed., McGraw-Hill, 2008, pp. 141-186.

[13] F. Beer, R. Johnston, J. Dewolf, and D. Mazurek, Appendix, *Mechanics of Materials*, Fifth ed., Mexico DF, McGraw Hill, 2010, pp. 735-763.

[14] A. Bayer, T. Vasco, and L. Walton, "Wrought tool steels," *Properties and Selection: Irons, Steels, and High-Performance Alloys*, ASM International, 1990, pp. 1764-1796.

[15] J. N. Perez, "Work, power and energy," B.S. thesis, Dept. Science Faculty., Univ National of Education Enrique Guzman y Valle., Lima, Peru, 2018.

[16] E. Martínez, "Calculation of helical compression springs," Cartagena, 2013.

[17] R. Budynas and K. Nisbett, "Mechanical springs," *Shigley´s Mechanical Engineering Design*, Eighth ed., McGraw Hill, 2008, pp. 499-549.

[18] K. Landines, N. Nieves, Y C. Toledo, "Simulation of forces applied to the human femur: analysis of finite elements," *Revista Vínculos: Ciencia, Tecnología y Sociedad*, vol. 16, no. 1, pp. 73-81, 2019.

[19] L. Dias, R. Magalhães, D. Ferreira, and A. Vitoriano, "The use of a robotic arm for displacement measurements in a cantilever beam," *International Journal of Manufacturing, Materials, and Mechanical Engineering*, vol. 6, no. 3, pp. 45-57, 2016.

[20] M. Weber and G. Verma, "NonLinear dynamic analysis," *SolidWorks Simulation 2017 Black Book*, CadCamCae Works, 2016, pp. 280-317.

[21] S. Gómez, "Motion study," The Big Book of SolidWorks, Alfaomega, 2015, pp. 393-427.

[22] A. Rustandi, S. Setiawan, M. Rendi, and Nuradityatama, "The use of cyclic polarization method for corrosion resistance evaluation of austenitic stainless steel 304L and 316L in aqueous sodium chloride solution," *International Journal of Mechanical Engineering and Robotics Research*, vol. 6, no. 6, pp. 512-518, 2017.

[23] S. Aslanzadeh *et. al.*, "Investigation on electrical and mechanical properties of 3D printed Nylon 6 for RF/Microwave electronics applications," *Additive Manufacturing*, vol. 21, pp. 69-75, 2018.

Carlos A. Toledo is a Professor of Industrial Engineering at the Francisco José de Caldas Distrital University. He is mechanical engineer from University of Los Andes, he has obtained his master in Industrial Engineering from University of Los Andes in 1999. Currently is a Ph.D Student in Engineering at the Francisco José de Caldas Distrital University. His research areas of interest include theory and applied mechanics and industry 4.0. ORCiD: 0000-0002-6437-092X.

Daniel S. Gordillo is student of engineering, Department of industrial engineering, Francisco José de Caldas Distrital University. Bogotá, Colombia. His current research interests include design and simulations of products and process.

Diego J. Sánchez born in Bogotá, Colombia in 1995, He is currently a student of industrial engineering, Department of industrial engineering, Francisco José de Caldas Distrital University. Bogotá, Colombia. He works like assistant of an investigation group GICALyT (Research group in supply chains, logistics and traceability). His research interests include manufacture design, project management and process planning.